Uncertainty Analysis of Dielectric Elastomers

Paul Miles
Advisor: William Oates
Mechanical Engineering, FAMU-FSU College of Engineering, Florida State University

Introduction:

- Dielectric elastomers (DE) have demonstrated promising properties for applications ranging from actuation, sensing, and energy harvesting [1]. By placing a compliant electrode on either side of these materials, one can apply voltage across the material thickness causing large electrostriction (i.e., electric field induced strain on the order of 100%).
- Considering the light weight properties of DE and its compact actuation mechanism, these soft materials are well suited for various platforms, including multi-modal legged robots, micro air vehicles, energy harvesting, biomedicine, and flexible electronics.
- Legged robots struggle to move on different surfaces as their components are typically designed for a single terrain. If a compliant structure could be incorporated into the leg mechanism, it could potentially allow for seamless transfer on to different terrains.
- In the area of flow control, one can similarly control the membrane's structure with an electrostatic field to alter the fluid-structure interactions. A more compliant membrane (as a result of electrostriction) will be significantly influenced by the surrounding flow physics.
- DE offer a route towards accomplishing these goals; however, adaptive structure designs and real-time control require accurate, robust, and numerically efficient predictions of the constitutive behavior and dynamic structure response. Whereas advanced electrostriction has been demonstrated, these elastomeric materials produce rate dependent behavior which has largely been neglected.

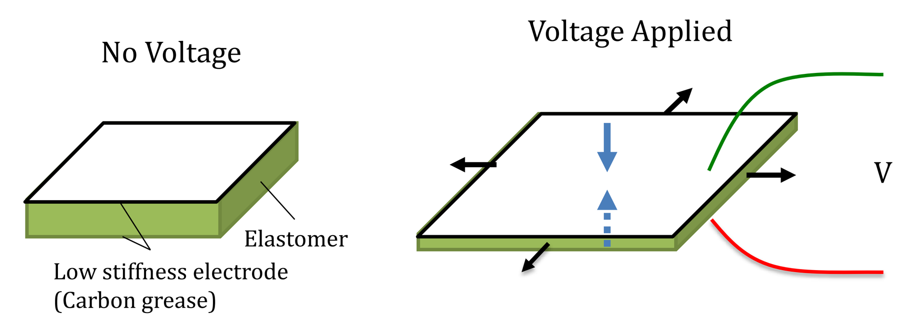

Figure 1: Activated electrodes compress, resulting in a decrease in tension and allowing for the outward expansion of the material.

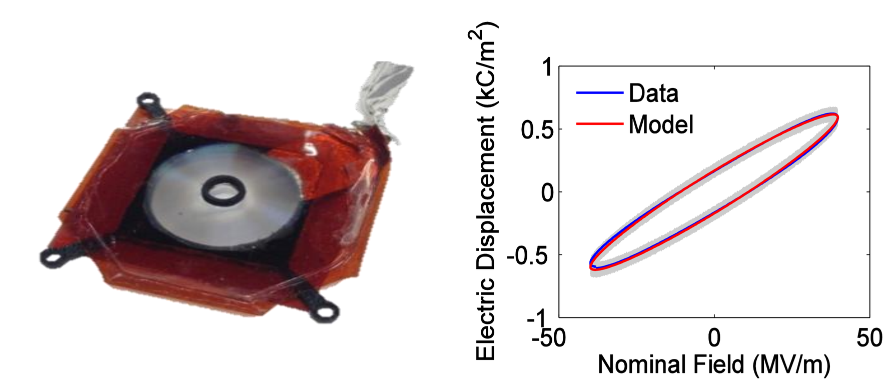

Figure 2: Model validation of electric displacement defined as a function of the nominal electric field [3].

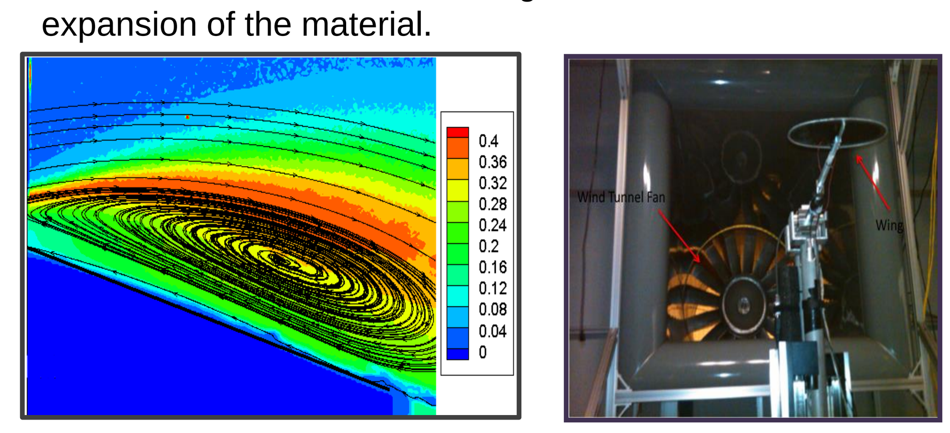

Figure 3: Wind tunnel testing of wing-shaped membrane [2].

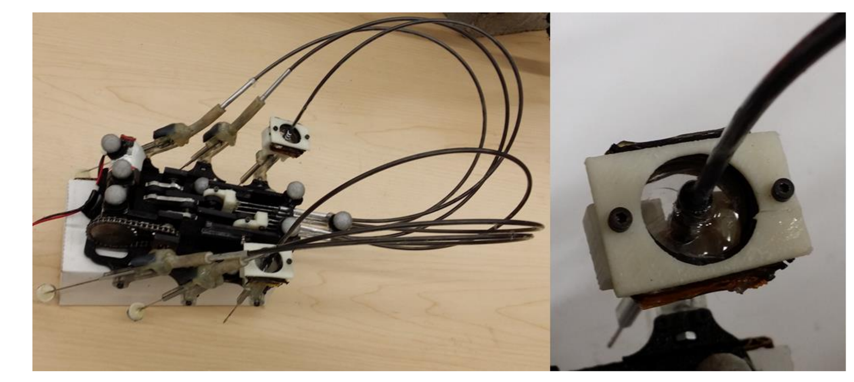

Figure 4: iSprawl robotic platform. Legs move up and down in such a way to provide forward motion.

Approach:

Beginning from a nonlinear rate-dependent model we integrate the constitutive equations into a finite deforming electroactive membrane structure. From there we compare with experiments and use Bayesian uncertainty quantification to assess model uncertainty and error propagation. We use information gained from the uncertainty analysis to reassess our material model and continue improving our overall structural model.

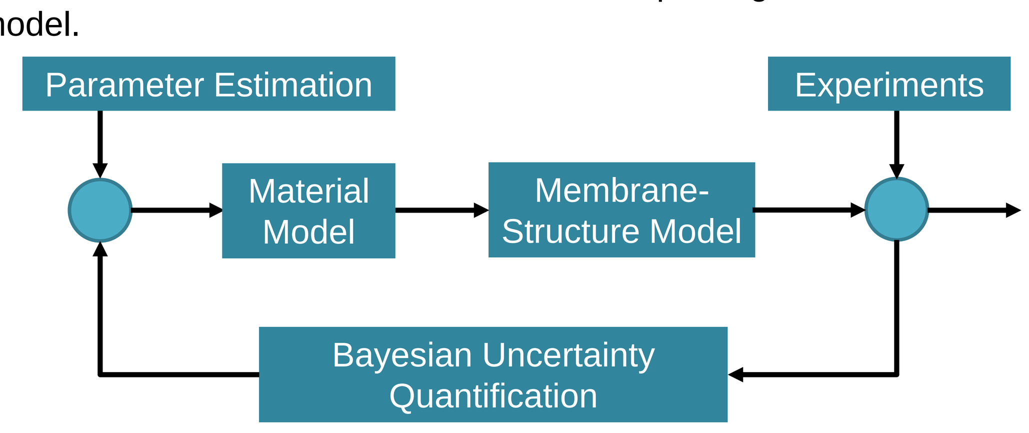

Figure 5: Flow chart for approach to model development.

Material Modeling:

Total Energy Density:

$$\psi = \psi_\infty(F_{iK},\theta) + \Upsilon(F_{iK},\theta,\Gamma_{iK}^{\alpha})$$

Total Stress:

$$s_{iK} = \frac{\partial\psi}{\partial F_{iK}} = \frac{\partial\psi_\infty}{\partial F_{iK}} - pJH_{iK} + \frac{\partial\Upsilon}{\partial F_{iK}}$$

Nonaffine Hyperelastic Free Energy [4]:

$$\psi_\infty^N = \frac{1}{6}G_c\lambda_{max}^2\log(3\lambda_{max}^2 - I_1) + G_e\sum_j\left(\lambda_j + \frac{1}{\lambda_j}\right)$$

where the invariant is $I_1 = \lambda_i\lambda_i$.

Nonlinear Viscoelastic Energy:

$$\Upsilon_{NL} = \sum_\alpha\left[\frac{1}{2}\gamma_\alpha\Gamma_{iK}^{\alpha}\Gamma_{iK}^{\alpha} - \beta_\infty^{\alpha}\frac{\partial\psi_\infty}{\partial F_{iK}}\Gamma_{iK}^{\alpha} + \beta_\infty^{\alpha}\psi_\infty\right]$$

Membrane Structure Modeling:

Transverse load [5]

$$F = 2\pi\sin(\theta)\,rt\sigma_l$$

where σ_l Cauchy stress in radial direction. Application of electric field in transverse direction decreases the Cauchy stress [5,6].

$$\sigma_l = \sigma_l^H - \kappa_r\epsilon_0E_t^2$$

Relative permittivity, κ_r, is assumed independent of deformation. The nonaffine hyperelastic stress is

$$\sigma_l^H = \frac{G_c}{3}\left(\lambda_{l,tot}^2 - \frac{1}{\lambda_{c,pre}^2\lambda_{l,tot}^2}\right)\left(\frac{9\lambda_{max}^2 - I_1}{3\lambda_{max}^2 - I_1}\right) + G_e\left(\lambda_{l,tot}(1+\lambda_{c,pre}) - \frac{1+\lambda_{c,pre}}{\lambda_{c,pre}\lambda_{l,tot}}\right)$$

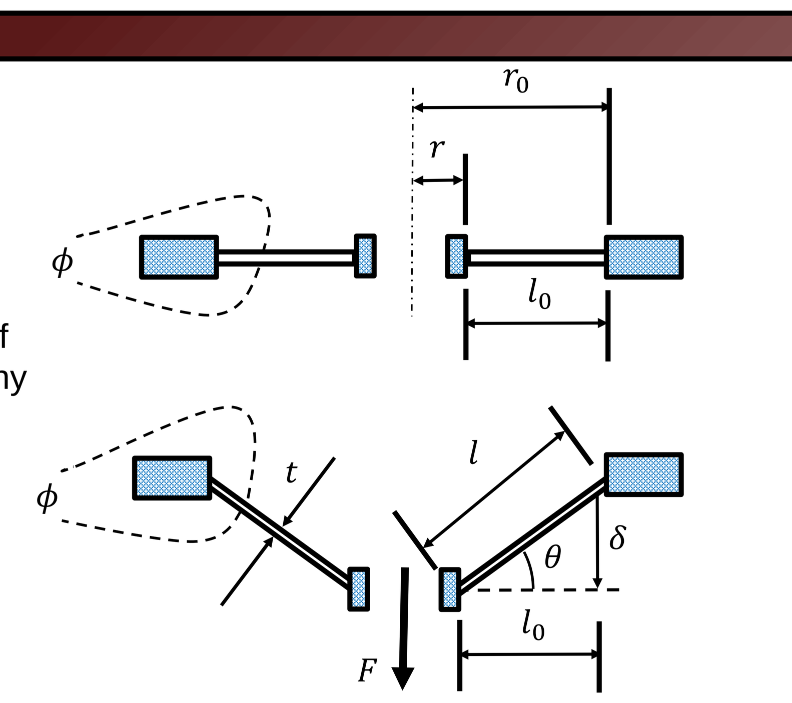

Figure 6: Membrane structure – a) Non-deformed configuration. b) Structure deformed a distance δ. Load response, F, is measured experimentally and modeled [3]. The electrostatic potential is denoted by ϕ.

Experiments:

- Uniaxial load/unload cycles using Very High Bond (VHB) 4910.
- Transverse loading of membrane structure (See Figure 6).
- Electric displacement measurements are taken on membrane structure in non-deformed configuration. Placed in Sawyer-Tower circuit with a known capacitor.

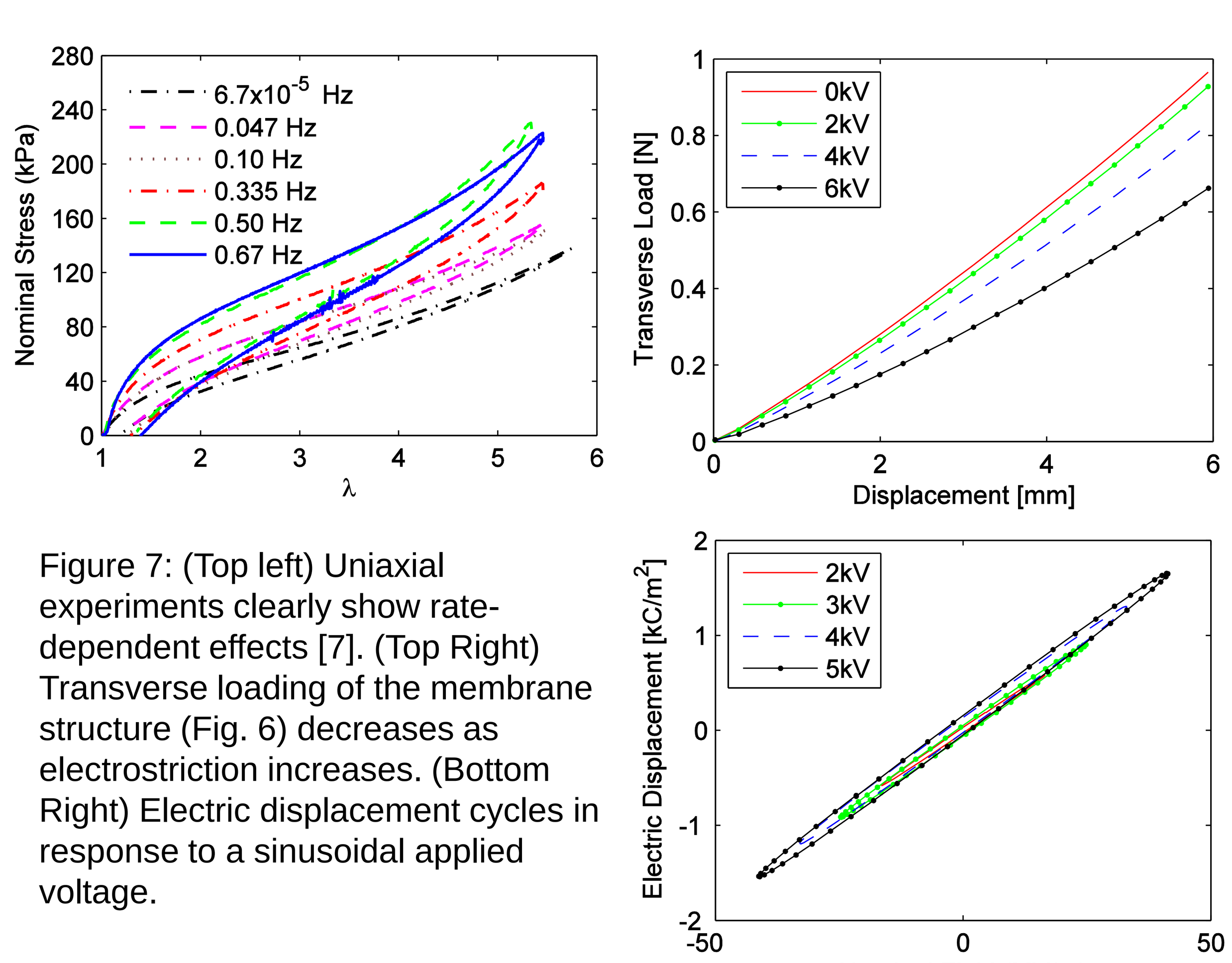

Figure 7: (Top left) Uniaxial experiments clearly show rate-dependent effects [7]. (Top Right) Transverse loading of the membrane structure (Fig. 6) decreases as electrostriction increases. (Bottom Right) Electric displacement cycles in response to a sinusoidal applied voltage.

Bayesian Uncertainty Quantification [8]:

Inverse problem using Bayes' Relation

$$\pi(\theta|M^{data}) = \frac{p(M|\theta)\pi_0(\theta)}{\int_{\mathbb{R}^p}p(M|\theta)\,\pi_0(\theta)d\theta}$$

$\pi(\theta|M^{data})$ - posterior density (distribution of parameter in light of data)
$\pi_0(\theta)$ - prior density (a priori knowledge about the parameter values)
$p(M|\theta)$ - likelihood of model given parameters

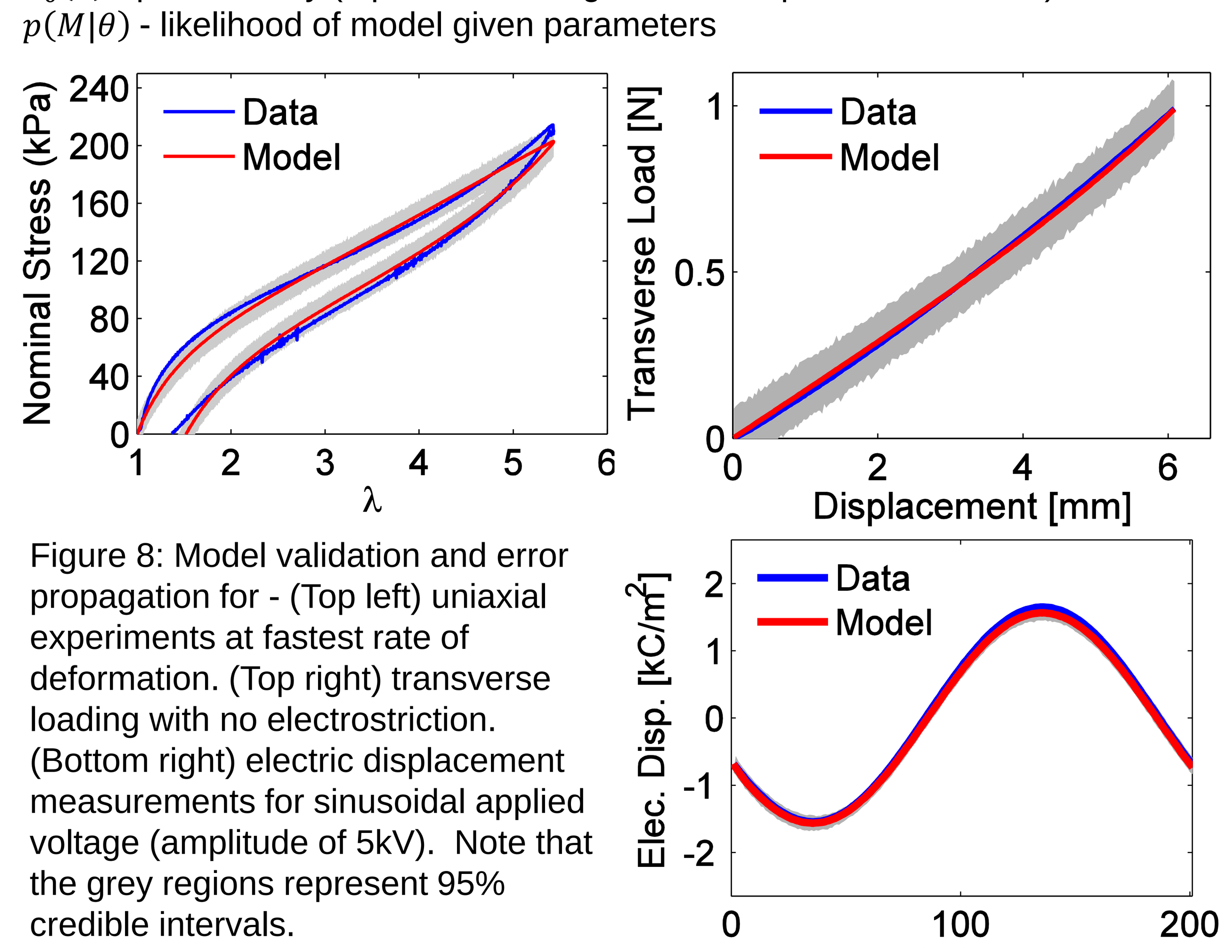

Figure 8: Model validation and error propagation for - (Top left) uniaxial experiments at fastest rate of deformation. (Top right) transverse loading with no electrostriction. (Bottom right) electric displacement measurements for sinusoidal applied voltage (amplitude of 5kV). Note that the grey regions represent 95% credible intervals.

Parameter Estimation:

Markov Chain Monte Carlo – MCMC
Assume unknown model parameters are random variables.

- Uniaxial, viscoelasticity model: $\theta = [G_c, G_e, \lambda_{max}, \gamma, \eta, \beta]$
- Transverse load model: $\theta = [G_c, G_e, \lambda_{max}, \kappa_r]$
- Electric displacement model: $\theta = [\kappa_r, \tau]$

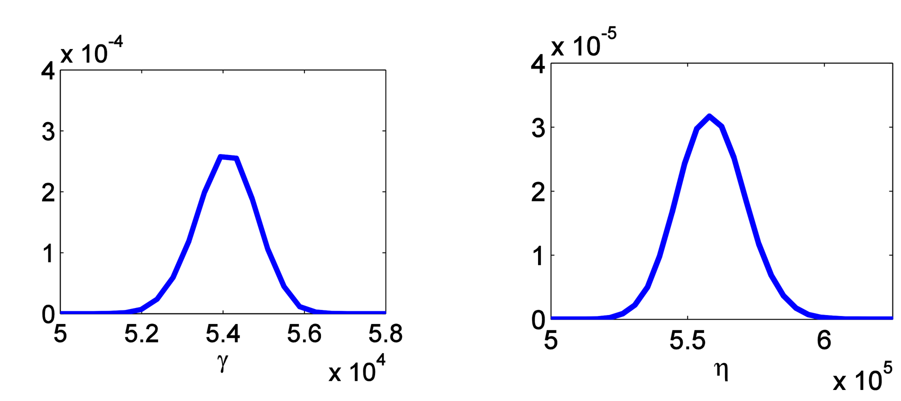

Figure 9: Bayesian posterior densities based on a nonlinear viscoelastic model (γ, η are shown as examples).

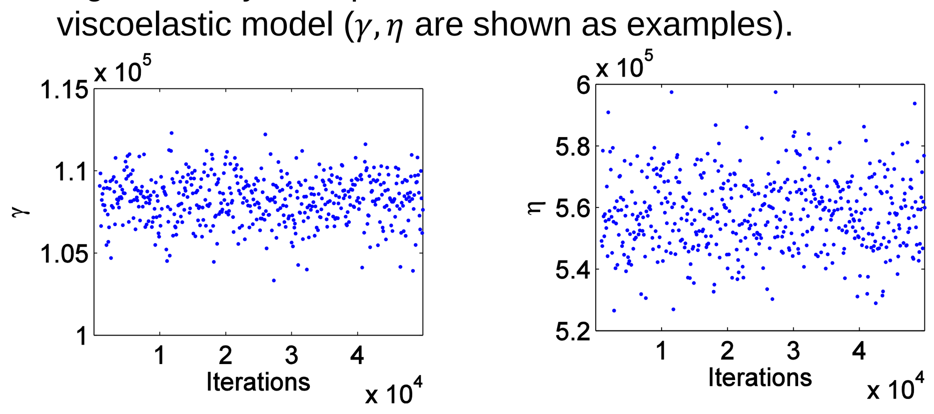

Figure 10: Chain panels based on a nonlinear viscoelastic model (γ, η are shown as examples). The plots show the space sampled during parameter estimation. The consistent bounds imply a converged solution.

Conclusion:

- It was shown that the nonlinear viscoelastic model quantified the rate-dependent deformation of VHB 4910 with the greatest accuracy, as it accounted for the behavior at all stretch rates with a single set of hyperelastic parameters.
- The time response of the nonlinear viscoelastic model follows a power law with respect to the deformation rate (See Figure 11). This opens up opportunities to explore origins for the power law based on the underlying polymer network physics.
- Uncertainty associated with model prediction in nonlinear rate dependent regimes is quantified using Bayesian statistics and its errors are propagated through the model to assess model accuracy with respect to experiments.
- These results show potential for applying controls to a robotic platform as the electrostrictive behavior causes significant change in the membrane stiffness as a function of applied field. Effective application of controls could assist a robot in adjusting to different terrains simply by applying different fields across the membrane.
- Determining the appropriate characteristics to enhance a robotic platform is currently under investigation to quantify fatigue behavior under electromagnetic loading. The use of Bayesian statistics is ideal to determine if posterior parameter densities evolve during fatigue which would lead to developments of more robust control algorithms and filter designs.

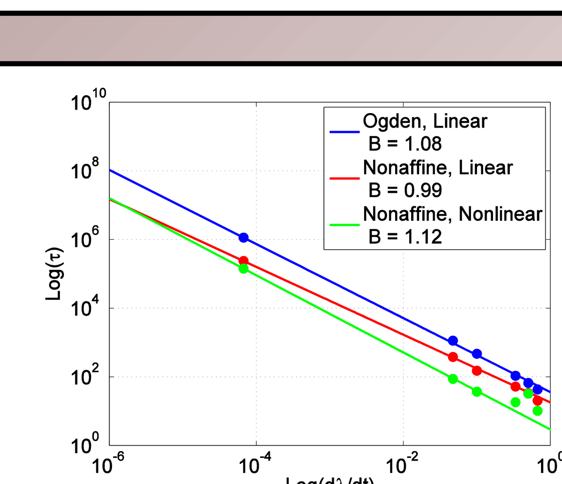

Figure 11: Power law viscoelastic behavior with respect deformation rate.

References:

[1] Anderson, et. al., 2012. "Multi-functional dielectric elastomer artificial muscles for soft and smart machines". *J. Appl. Phys.*, 112, p. 041101.

[2] Hays, et al. "Aerodynamic Control of Micro Air Vehicle Wings Using Electroactive Membranes," J. Mater. Syst. Struct., v. 24(7), pp. 862-878, 2013.

[3] Miles, Paul, et al. "Uncertainty Analysis of Dielectric Elastomer Membranes Under Multi-Axial Loading." ASME 2015 Conference on Smart Materials, Adaptive Structures and Intelligent Systems, 2015.

[4] Davidson, et al. "A nonaffine network model for elastomers undergoing finite deformations." Journal of the Mechanics and Physics of Solids 61.8 (2013): 1784-1797.

[5] Rizzello, et al. "Dynamic Electromechanical Modeling of a Spring-Biased Dielectric Electroactive Polymer Actuator System." ASME 2014 Conference on Smart Materials, Adaptive Structures and Intelligent Systems, 2014.

[6] Zhao, et al. "Electromechanical hysteresis and coexistent states in dielectric elastomers." Physical review B 76.13 (2007): 134113.

[7] Miles, et al. "Bayesian uncertainty analysis of finite deformation viscoelasticity." Mechanics of Materials 91 (2015): 35-49

[8] Smith, *Uncertainty quantification: theory, implementation, and applications*. Vol. 12. SIAM, 2013.

Acknowledgements:

WSO and PRM gratefully acknowledge support from an Army Research Laboratory Collaborative Technology Alliance (R-CTA) and the Army Research Office through Grant W911NF-13-1-0146, program manager Matthew Munson. WSO also appreciates NSF support through the Collaborative Research CMMI Grant 1306320. Special thanks to the students who have contributed to this research: Adriane Moura, Wei Gao, and Justin Collins.